Physicochemical Parameters Responsible for the Affinity of Methotrexate Analogs for Rat Canalicular Multispecific Organic Anion Transporter (cMOAT/MRP2)

Yong-Hae Han,[1,3] Yukio Kato,[1] Masayuki Haramura,[2] Masateru Ohta,[2] Hiroharu Matsuoka,[2] and Yuichi Sugiyama[1,4]

Received January 25, 2001; accepted February 5, 2001

Purpose. Canalicular multispecific organic anion transporter (cMOAT/MRP2) is known to exhibit a broad substrate specificity toward amphiphatic organic anions, including methotrexate (MTX). The present study aims to identify the physicochemical properties of MTX derivatives that correlate with recognition specificity by cMOAT/MRP2.

Methods. We examined the inhibitory effect of MTX and 24 analogs on the transport of [^{3}H]-S-(2,4-dinitrophenyl)glutathione by cMOAT/MRP2. The affinity constants of these compounds were compared with their physicochemical parameters. The primary active transport of several compounds was also confirmed.

Results. The affinity constants closely correlated with the octanol/water partition coefficient (clogP), and a linear combination of polar and nonpolar surface areas. The affinity for cMOAT/MRP2 also closely correlated with the molecular weight, which also showed a significant correlation with nonpolar surface area and clogP.

Conclusions. Recognition by cMOAT/MRP2 depends on a balance of dynamic surface properties between the polar and nonpolar regions of MTX analogs. The so-called "molecular weight threshold" for the cMOAT/MRP2 affinity of these compounds can be explained by their physicochemical parameters, especially their nonpolar surface areas.

KEY WORDS: cMOAT/MRP2; primary active transport; octanol/water partition coefficient; dynamic molecular surface area; substrate specificity.

INTRODUCTION

Long-term methotrexate (MTX) therapy is associated with serious side effects, such as nephrotoxicity and altered hepatic function (1,2). Such toxicity is believed to stem from its long-term accumulation in tissues, and there is an urgent need for new derivatives that are less likely to accumulate. Knowledge of the factors contributing to the tissue accumulation will provide a solid basis for the design and synthesis of such novel antifolate compounds (3,4). Approximately 10–30% of MTX is eliminated by an active transport mechanism through biliary excretion and subsequent enterohepatic circulation (5). We have shown that MTX is excreted into bile via the canalicular multispecific organic anion transporter (cMOAT/MRP2), which is an apical isoform of the multidrug resistance associated protein family (6). Apart from its intracellular binding to target enzymes, such as dihydrofolate reductase, the transport of MTX by cMOAT/MRP2 should also be a key factor in determining its intrahepatocellular retention.

cMOAT/MRP2 transports a variety of compounds (7,8), most of the cMOAT/MRP2 substrates being organic anions, but compounds of the zwitterionic type like MTX, are also substrates (6). Reduced glutathione, small peptides, and other nonconjugated organic anions are also recognized by cMOAT/MRP2 (7,8). Thus, the determining factor governing the recognition of substrates by cMOAT/MRP2 remains to be identified. To investigate the physicochemical properties involved in the affinity for cMOAT/MRP2, in the present study, we examined the inhibition of cMOAT/MRP2 by MTX and 24 novel antifolate compounds (Fig. 1). To identify the most important parameters for cMOAT/MRP2 recognition, we examined the correlation between the inhibitory effect, assessed as the inhibition constant (K_i), and physicochemical parameters, including the dynamic molecular surface properties which have recently been reported by Parm *et al.* and Stenberg *et al.* (9–11).

MATERIALS AND METHODS

Materials

[^{3}H]-S-(2,4-dinitrophenyl) glutathione ([^{3}H]-DNP-SG, 50.0 μCi/nmol) was synthesized as described previously (6). MTX was purchased from Sigma Chemical Corp (St. Louis, MO). MTX analogs were synthesized at Chugai Pharmaceutical Company (Shizuoka, Japan).

Uptake of DNP-SG by CMVs

Male Sprague–Dawley rats (Nisseizai, Tokyo, Japan) weighing 250–300 g were used. This study was carried out in accordance with the Guide for the Care and Use of Laboratory Animals as adopted and promulgated by the US National Institutes of Health. The transport medium containing [^{3}H]DNP-SG (1 μM) or 1 μM [^{3}H]DNP-SG and unlabeled MTX analogs (1–1000 μM) were preincubated for 3 min and then incubated with CMVs for 2 min (6). Uptake was normalized with respect to both the medium concentration of substrates and the amount of membrane protein. The ATP-dependent uptake was assessed by subtracting the uptake in the presence of AMP from that in the presence of ATP.

Determination of the Uptake of #18, #20, #10, #16, and MTX

After washing CMVs loaded on the membrane filter (6), the filters were dried and cut into small pieces. The drug was extracted with 63% MeOH containing internal standard (IS). After centrifugation, the supernatant was evaporated, dissolved in 10 mM ammonium acetate (pH 9.0) and injected onto an HPLC column (Capcell Pak UG120, Shiseido, Yo-

[1] Graduate School of Pharmaceutical Sciences, University of Tokyo, 7-3-1, Hongo Bunkyo-ku, Tokyo, 113-0033, Japan.
[2] Chemistry Research Laboratory, Fuji Gotemba Research Laboratories, Chugai Pharmaceutical Co., Ltd., 1-135 Komakado, Gotemba-shi, Shizuoka 412-8513, Japan.
[3] Present address: Renal Pharmacology Section, MD:F2-03, LPC, NIEHS/NIH, PO Box 12233, RTP, North Carolina 27709.
[4] To whom reprint requests should be addressed. (e-mail: BXG05433@niftyserve.or.jp)

0724-8741/01/0500-0579$19.50/0

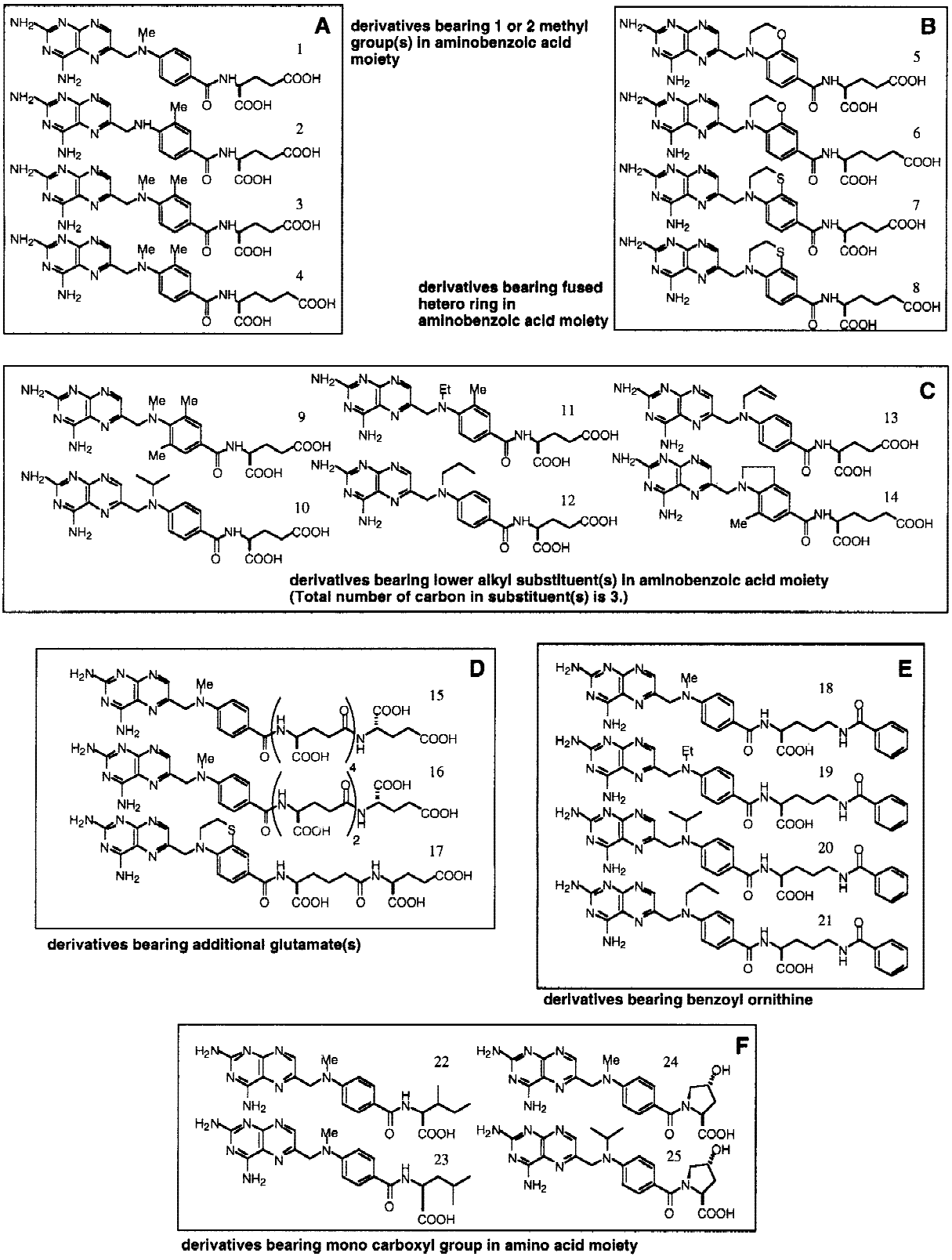

Fig. 1. Molecular structure of MTX analogs.

kohama, Japan). The mobile phase consisted of A: 5% MeOH in 10 mM ammonium acetate (pH 9.0), B: 80% MeOH in 10 mM ammonium acetate (pH 9.0). The mobile phase gradient was as follows: 10% to 95% mobile phase B in A from 0 to 5 min, 95% mobile phase B in A from 5 to 6 min, 95% to 10% mobile phase B in A from 6 to 8 min, and 10% mobile phase B in A from 8 to 13 min. The flow rate was 0.05 ml/min. The IS was #18 for the assay of #20, #10, #16, and

MTX whereas the IS was #20 for the assay of #18. Each compound was detected by mass spectrometry (LCQ, ThermoQuest, San Jose, CA, USA).

Estimation of Kinetic Parameters

Uptake of DNP-SG was fitted to the Michaelis-Menten equation to obtain the Michaelis constant (K_m) and the maximum uptake rate (V_{max}). The K_i of MTX analogs was estimated by fitting the ratio of ATP-dependent [^{3}H]DNP-SG uptake in the presence of MTX analog ($V_{o(+inhibitor)}$) at a concentration of I to that in its absence ($V_{o(-inhibitor)}$) using the following equation (6):

$$V_{o(+inhibitor)}/V_{o(-inhibitor)} = 1/(1 + I/K_i) \quad (1)$$

Calculation of Physicochemical Parameters

The three-dimensional structures of the compounds were determined by using the random search module included in the molecular modeling package, SYBYL version 6.4 (Tripos Inc., St. Louis, MO). The algorithm of the program GEPOL (QCPE554) (12,13) was used for the surface area calculation. The polar surface area (PSA_d) was defined as the area occupied by nitrogen and oxygen atoms, as well as hydrogen atoms attached to these heteroatoms. The non-polar surface area ($NPSA_d$) was defined as the area occupied by carbon atoms and hydrogen atoms attached to carbon atoms. Theoretical estimates of clogP were made using CLOGP version 4.41 (Daylight C. I. S., Inc., Rochester, NY, USA).

Data Analysis

Linear regression was performed using Excel 97 for Macintosh. Multiple regression analysis was performed for the linear combination of PSA_d and $NPSA_d$. A p value of less than 0.05 was considered to be statistically significant.

RESULTS

Inhibition of ATP-Dependent DNP-SG Uptake by MTX Analogs

The enrichment of Mg^{2+} ATPases and alkaline phosphatase in CMVs, compared with liver homogenate, was 97.6 ± 9.5 and 75.3 ± 6.9, respectively (mean ± SE of three determinations). The K_m and V_{max} for the ATP-dependent uptake of [^{3}H]DNP-SG (13.2 ± 0.9 μM and 756 ± 27 pmol/min/mg protein, respectively) were comparable with our previous data (6). DNP-SG uptake was inhibited by MTX analogs. A typical inhibition curve is shown in Fig. 2. More than a 70-fold difference was observed among these K_i values (Table I).

Primary Active Transport of MTX Analogs

The uptake of #18 and #20, which showed a relatively higher inhibitory effect on DNP-SG uptake (Table I), was stimulated by ATP (Fig. 3). Their uptake profiles in the presence of ATP showed overshoot phenomena (Fig. 3). The uptake of #10, #16, and MTX for 2 min was also stimulated by ATP (Fig. 3). The rank order of the ATP-dependent uptake was #20 > #10 ≥ #18 > MTX > #16 (54.7 ± 12.7, 11.7 ± 7.9, 10.9 ± 1.0, 5.14 ± 1.94, and 0.923 ± 0.468 μl/mg, respectively).

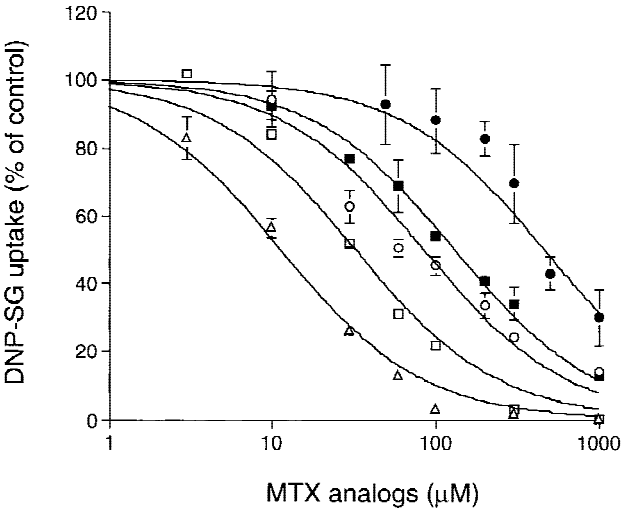

Fig. 2. Typical inhibition curves for a series of MTX analogs on ATP-dependent DNP-SG uptake by CMVs. Data represent the mean ± SE of three determinations in two preparations. The fitted line based on Eq. (2) is also shown. #11 (○), #7 (■), #19 (□),#21 (△), MTX (●).

Correlation Between the Affinity for cMOAT/MRP2 and the Physicochemical Parameters of Each MTX Analog

The correlation between the affinity constant, assessed as the reciprocal of K_i ($1/K_i$), for cMOAT/MRP2 with the clogP

Table I. Physicochemical Parameters and cMOAT/MRP2 Affinity of MTX Analogs

Compound no.	Mw[a]	clogP[b]	PSA_d (A^2)[c]	$NPSA_d$ (A^2)[d]	Ki (μM)[e]
1	454.5	–0.87	294	309	462
2	454.5	–1.71	332.4	261.8	382
3	468.5	–0.37	367.7	305.4	150
4	482.5	0.16	311.2	344.6	133
5	482.5	–0.69	381.8	318	311
6	496.5	–0.16	313.2	290.8	204
7	498.5	–0.27	306	321.8	137
8	512.6	0.26	313	367	159
9	482.5	0.13	309.6	352.5	39.2
10	482.5	–0.19	334	322	173
11	482.5	0.58	329.2	342.1	98.3
12	482.5	0.03	389	359	154
13	480.5	–0.45	308	354	136
14	512.6	0.01	295	329.9	173
15	969.9	–3.48	550	565	501
16	712.7	–1.91	439	422	838
17	641.7	–1.05	344	407	223
18	543.6	0.76	223	416	48.7
19	557.6	1.21	256	456	32.5
20	571.6	1.47	303	452	14.8
21	571.6	1.66	248	501	11.4
22	438.5	1.52	205	397	56.9
23	438.5	1.52	230	389	308
24	438.4	–0.68	279	294	>1000
25	466.5	–0.01	284	334	784

[a] Molecular weight.
[b] Calculated octanol/water partition coefficient.
[c] Polar surface area (N, O, H atoms).
[d] Nonpolar surface area.
[e] Inhibition constant for the transport of DNP-SG by cMOAT.

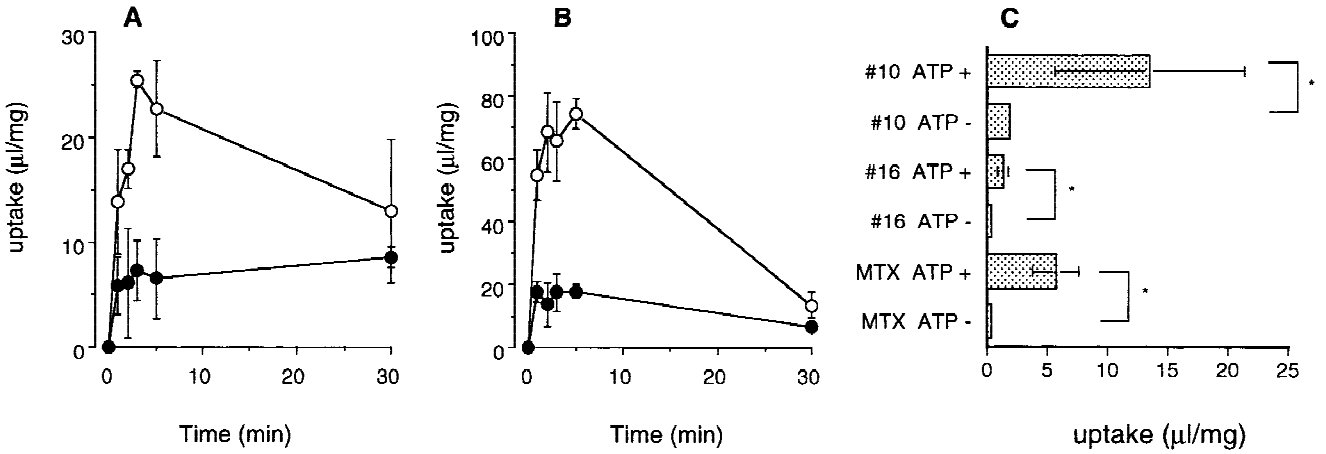

Fig. 3. Uptake of #18, #20, #10, #16, and MTX (#1) by CMVs. (A and B) Uptake of #18 (A) and #20 (B) at 10 μM was determined in the presence of ATP (○) or AMP (●). (C) Uptake of #10, #16, and MTX at 10 μM during a 2-min incubation was determined in the presence of ATP or AMP. Data represent the mean±SE of 3 determinations in 1 preparation. * Significantly different from the uptake in the absence of ATP ($P < 0.05$).

and molecular weight (Mw) was examined (Fig. 4). As the clogP increased, the $1/K_i$ also tended to increase (Fig. 4A, inset). A significant correlation was observed between the logarithm of $1/K_i$ with clogP (Fig. 4A, Table IIB). A higher $1/K_i$ was observed for the four analogs with an Mw of 540–580, whereas three polyglutamate compounds (#15, #16, and #17) exhibited a much lower $1/K_i$ (Fig. 4B, inset). Since these polyglutamates have an Mw outside the range studied (M_w > 640, Fig. 4B), the correlation analysis was performed for two cases, where three such compounds were included or not (Table 2). Except for three compounds, a significant correlation was also found between $\log(1/K_i)$ and M_w (Fig. 4B, Table IIA). A minimal correlation was found between $1/K_i$ and PSA_d (Fig. 5A, inset). A correlation with $1/K_i$ or $\log(1/K_i)$ and $NPSA_d$ was also minimal if all the analogs were included in the regression analysis (Fig. 5B, Table IIB) whereas, if the three polyglutamate compounds were excluded, a reasonable correlation was observed between $\log(1/K_i)$ and $NPSA_d$ (Fig. 5B, Table IIA).

Linear Regression Analysis

Linear regression analysis was performed between $\log(1/K_i)$ and clogP, PSA_d, $NPSA_d$, or M_w (Table II). Significant

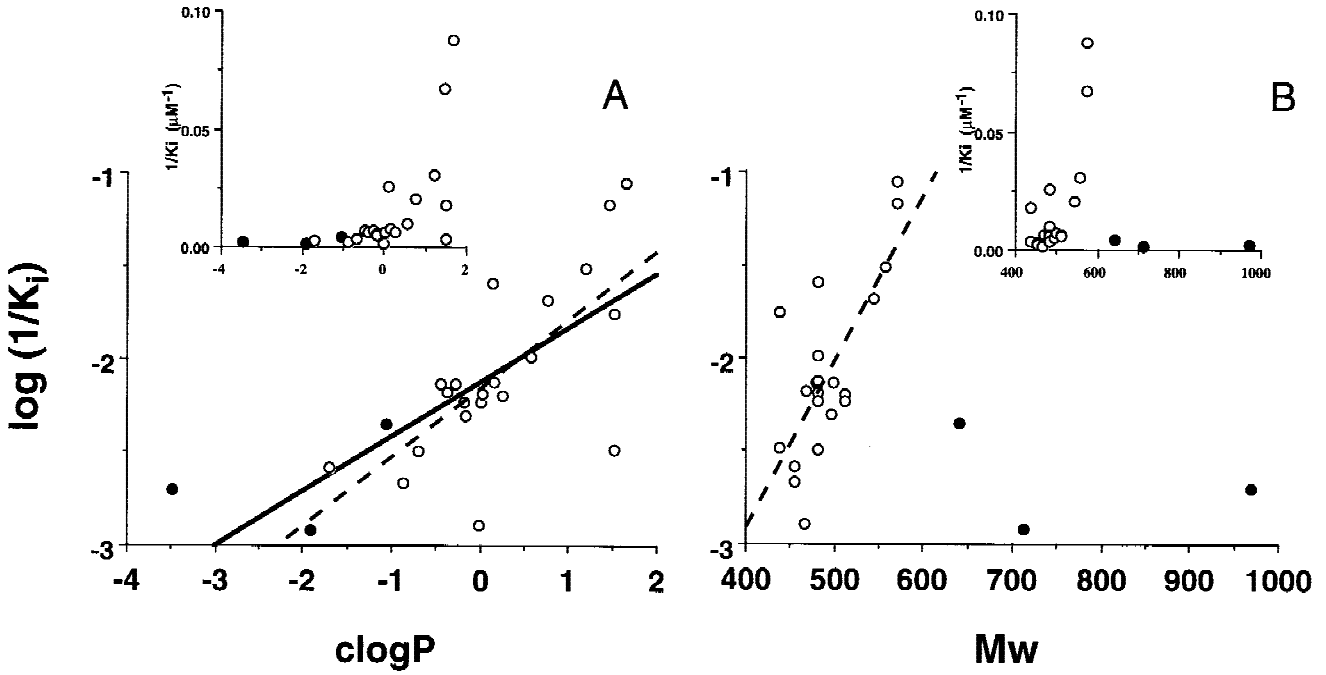

Fig. 4. Relationship between the affinity constant for cMOAT/MRP2 ($1/K_i$) and clogP or molecular weight. The logarithm of $1/K_i$ for MTX analogs was plotted against the clog P (A) or M_w (B). The correlation for the normal scale of $1/K_i$ is also shown as an inset. Polyglutamate compounds are shown as closed symbols. The straight and broken lines represent the significant correlation lines for all MTX analogs and MTX analogs except the polygrutamates, respectively.

Table II. Correlation Coefficient and Linear Regression Between Physicochemical Parameters and Affinity for cMOAT/MRP2[a]

(A) Without compounds #15, 16, and #17

	$\log(1/K_i)$	clogP	PSAd	NPSAd	M_w
$\log(1/K_i)$	1				
clogP	0.690[c,d]	1			
PSAd	–0.0928	–0.316	1		
NPSAd	0.811[c,d]	0.877[c,d]	–0.330	1	
M_w	0.741[c,d]	0.449[b,d]	–0.0757	0.689[c,d]	1

(B) For all compounds

	$\log(1/K_i)$	clogP	PSAd	NPSAd	M_w	Linear combination[f]
$\log(1/K_i)$	1					
clogP	0.716[c,e]	1				
PSAd	–0.349	–0.680[c,e]	1			
NPSAd	0.351	0.0252	0.275	1		
M_w	–0.145	–0.588[c,e]	0.675[c,e]	0.759[c,e]	1	
Linear combination[f]	0.581[c]	–0.584[c]	0.599[c]	–0.605[c]	0.0737	1

[a] Correlation coefficient (r) is shown.
[b] $P < 0.05$.
[c] $P < 0.01$.
[d] The significance ($P < 0.05$) in linear regression was observed; $\log(1/K_i) = -2.16 + 0.368 \times$ clogP, $-4.39 + 0.00647 \times NPSA_d - 6.46 + 0.00887 \times$ Mw; clogP $= -4.49 + 0.0131 \times NPSA_d$, $-4.77 + 0.0101 \times$ clogP; $NPSA_d = -152 + 1.03 \times M_w$.
[e] The significance ($P < 0.05$) in linear regression was observed; $\log(1/K_i) = -2.13 + 0.290 \times$ clogP, $3.00 - 0.00996 \times PSA_d$, $3.21 - 0.00622 \times M_w$; $PSA_d = 51.0 + 0.487 \times M_w$; $NPSA_d = 123 + 0.471 \times M_w$.
[f] $\text{Log}(1/K_i) = -2.51 - 0.00286 \times$ PSAd $+ 0.00335 \times$ NPSAd ($P < 0.05$).

regression was observed only between $\log(1/K_i)$ and clogP (Table II) when all the compounds were used in the analysis. When three polyglutamates were excluded, there was a significant correlation between $\log(1/K_i)$ and clogP, $NPSA_d$, or M_w (Table II). These three parameters were all correlated whereas only a minimal correlation was found between PSA_d and $NPSA_d$ (Table II). Multiple regression analysis was performed between $\log(1/K_i)$ and a linear combination of PSA_d and $NPSA_d$ (Table II). Such regression analyses were significant when all the MTX analogs were included in the analysis (Table II, Fig. 5C). The correlation of such linear combinations with $\log(1/K_i)$ was significant (Table II), but not very marked (Fig. 5C).

DISCUSSION

Because MTX can sometimes alter hepatic function because of its accumulation in the liver, we designed derivatives in the present study to identify those analogs exhibiting a lower degree of liver accumulation. These derivatives have more than one carboxyl group, leading us to consider the possibility that these compounds may also be substrates and/or inhibitors of cMOAT/MRP2. To examine this possibility, we first examined their effectiveness as inhibitors of the transport of a typical substrate by cMOAT/MRP2. The broad range of affinity of these compounds suggests that there is a structural requirement in these MTX derivatives for a high degree of interaction with cMOAT/MRP2.

A significant degree of correlation and linear regression were found between $\log(1/K_i)$ and clogP (Fig. 4A). Thus, the lipophilicity of MTX analogs increased their inhibition potency as in the case of recognition by other receptors, transporters or serum proteins e.g. between 5-HT_{1A} receptors and eltoprazine derivatives (14), P-glycoprotein and anthracycline analogs (15) or several organic cations (16), albumin, and penicillin analogs (17). However, lipophilicity does not always correlate with receptor affinity. No correlation was found between the lipophilicity of histamine H_2 receptor antagonists and their receptor affinity (18). Also no significant correlation has been found between the lipophilicity of oxytocin analogues and their binding affinity for myometrial receptors (19).

To identify other physicochemical properties correlating more closely with cMOAT/MRP2 affinity, we examined the dynamic surface area which reflects the three-dimensional shape and conformational flexibility of the compounds (9–11). Only a minimal correlation was found between $\log(1/K_i)$ and PSA_d or $NPSA_d$ if we included all the compounds examined (Fig. 5). Nevertheless, $NPSA_d$ correlates with $\log(1/K_i)$ for all MTX analogs except three polyglutamates (Fig. 5B). Thus, $NPSA_d$ is one of the parameters describing the cMOAT/MRP2 affinity for certain types of analogs. The three polyglutamates have a higher PSA_d and lower $\log(1/K_i)$ than other analogs (Fig. 5A). Such a higher PSA_d may reduce their affinity. Considering a minimal correlation between PSA_d and $NPSA_d$, we then carried out a multiple regression analysis between $\log(1/K_i)$ and a linear combination of these two parameters (Table II). A degree of significance was observed in such an analysis (Table II), suggesting that the balance of these two parameters may account for the cMOAT/MRP2 affinity of all MTX analogs. This implies that the hydrophilic surface area in polyglutamates hinders recognition by cMOAT/MRP2 whereas the hydrophobic surface area increases the cMOAT/MRP2 affinity. Such a combination of these two surface properties may be compatible with the recent finding that most of the cMOAT/MRP2 substrates are anionic and hydrophobic in nature (7,8). However, the cor-

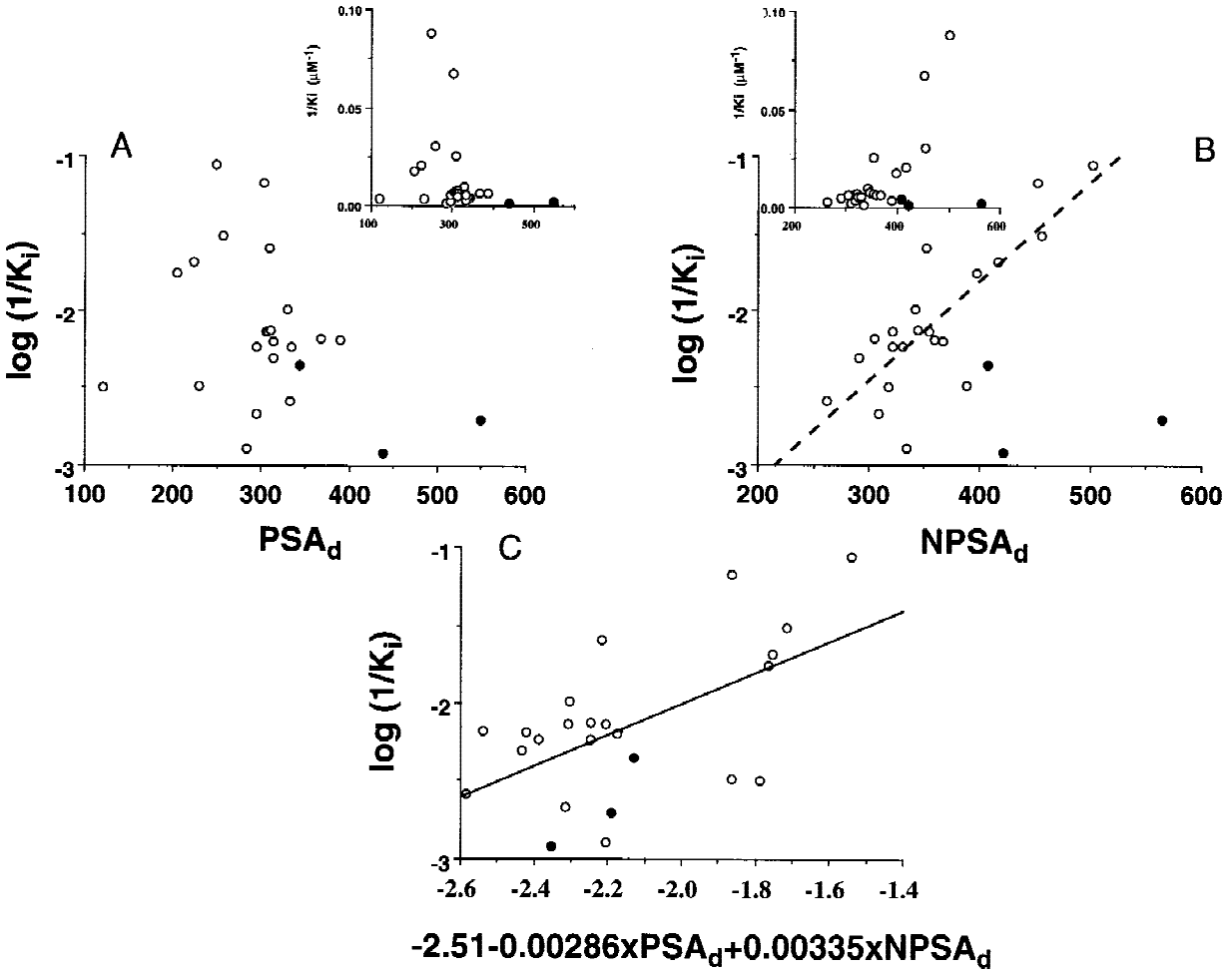

Fig. 5. Relationship between the affinity constant for cMOAT/MRP2 ($1/K_i$) and dynamic molecular surface. The logarithm of $1/K_i$ for MTX analogs was plotted against the PSA_d (A), $NPSA_d$ (B), or their combination (C). The correlation for the normal scale of $1/K_i$ is also shown as an inset. The polyglutamate compounds are shown as closed symbols. The straight and broken lines represent the significant correlation lines for all MTX analogs and MTX analogs except the polygrutamates, respectively.

relation between $\log(1/K_i)$ and the linear combination (Fig. 5C) or clogP (Fig. 4A) for all MTX analogs is still not very apparent (Fig. 5C), suggesting that the cMOAT/MRP2 affinity cannot be fully explained by these parameters.

The $1/K_i$ may not be sufficient to define cMOAT/MRP2 recognition since the inhibitory compounds may or may not be actually transported by cMOAT/MRP2. To obtain an insight into the relationship between the physicochemical parameters and cMOAT/MRP2-mediated transport, we measured the ATP-dependent uptake of five MTX compounds with a range of K_i values (15–840 μM) which almost covers the observed K_i values for all the MTX analogs examined (Table I). The rank order of the $1/K_i$ was essentially compatible with their ATP-dependent uptake (Fig. 3, Table I). If we assume that the K_i for inhibition is equal to the K_m for transport, the transport clearance found in this study should represent the V_{max}/K_m or at least half the V_{max}/K_m since the substrate concentration in this transport study was much lower than the K_i for #18, #10, MTX, and #16 and almost comparable with the K_i for #20. Therefore, the parallelism between the transport clearance and $1/K_i$ (or $1/K_i$) should indicate that the difference in transport activity among these compounds can be accounted for mainly by the difference in K_i value. Thus, although further studies should be performed to confirm that all MTX analogs are substrates of cMOAT/MRP2, the present findings suggest that the transport activity of cMOAT/MRP2 can be described primarily by clogP or the dynamic nonpolar surface area of each compound. Bain and LeBlanc (20) reported that both lipophilicity and molecular mass are the major determinants of the binding of pesticides to P-glycoprotein, with optimum binding occurring with compounds having a log octanol-water-partition of 3.6–4.5 and an M_w of 391–490 Da. On the other hand, there seemed to be no optimal value for clogP or Mw as far as affinity for cMOAT/MRP2 was concerned (Fig. 4). However, the clogP and Mw of the MTX analogs were at most 1.7 and mainly within the range 440–570, respectively (Table I). Therefore, further studies will be needed using other types of compounds with higher lipophilicity as well as wider range of Mw to examine their optimum values in terms of transport activity by cMOAT/MRP2. The $\log(1/K_i)$ for cMOAT/MRP2 did not correlate with the reciprocal of their half-inhibitory concentration for the growth of human peripheral mononuclear cells (21,22), suggesting that it may be possible to design MTX

analogs exhibiting optimum recognition by cMOAT/MRP2 and intrahepatocellular accumulation with anti-dehydrofolate reductase activity.

There may be a molecular weight threshold for compounds efficiently excreted into the bile (23,24). Although the $\log(1/K_i)$ was higher for the compounds with a higher Mw (Fig. 4B), further studies are needed to conclude that the M_w is the main factor determining whether MTX analogs undergo biliary excretion since the M_w also correlates well with $NPSA_d$, as does clogP to a lesser extent (Table II). Such a correlation means that derivatization of MTX analogs results in an increase both in the molecular size and lipophilicity.

In order to investigate the qualitative structural requirements for recognition by cMOAT/MRP2, we have structurally divided MTX derivatives into 6 classes (Fig 1). In Group A, the K_i of #3, having 2 carbon substituents on the central moiety, was 2–3 times lower than that of 1 or 2, having only one carbon (Table I). Such enhancement of the affinity with an increase in the number of carbons in the central moiety, has often been found in other derivatives in Groups A, C and E (Table I), suggesting that the MTX derivatives undergo a hydrophobic interaction with cMOAT/MRP2 via the central moiety. The K_i values of glutamate derivatives #3, #5, and #7 were comparable with those of homoglutamate counterparts #4, #6, and #8, respectively, in Groups A and B (Table I), suggesting that the hydrophobicity of the terminal amino acid moiety of the derivatives may not, in contrast, be critical for interaction with cMOAT/MRP2. Ornithine derivatives #18, #19, #20, and #21 in Group E have very low K_i (Table I). The key structural features of the ornithine derivatives, compared with the others, include the presence of a terminal extended volume and the absence of an acidic carboxyl group in the amino acid moiety. This suggests the existence of hydrophobic π–π or van der Waals interactions between the terminal moiety of the ornithine derivatives and cMOAT/MRP2. This hypothetical interaction would help explain the high K_i values of derivatives with an acidic, hydrophilic terminal moiety, i.e. #15, #16, and #17 in Group D (Table I). As far as #22, #23, #24, and #25 in Group F are concerned, no qualitative structural relationship was found, and the hypothetical terminal interaction could not explain the wide-range of K_i values (Table I). Further derivatizations and evaluations may be required for a complete analysis of the structure relationship in this group as well as a final demonstration of the above hypothesis.

In conclusion, the present analysis shows that recognition by cMOAT/MRP2 depends on a balance between the dynamic polar and nonpolar surface properties of MTX analogs. The physicochemical parameters, especially their $NPSA_d$, of MTX analogs can, at least partly, account for the molecular weight threshold as far as their affinity for cMOAT/MRP2 is concerned.

ACKNOWLEDGMENTS

This work was supported in part by a Grant-in-Aid for Scientific Research on Priority Area (A) "Molecular Synchronization for Design of New Materials System" provided by the Ministry of Education, Science and Culture of Japan and in part by TBRF (Tokyo Biochemical Research Foundation). We are grateful to Dr Motohiro Kato, Chugai Pharmaceutical Co., Ltd. for helpful discussion of the statistical analysis.

REFERENCES

1. B. Bannwarth, F. Pehourcq, T. Schaeverbeke, and J. Dehais. Clinical pharmacokinetics of low-dose pulse methotrexate in rheumatoid arthritis. *Clin. Pharmacokin.* **30**:194–210 (1996).
2. M. E. Weinblatt, B. N. Weissman, D. E. Holdsworth, P. A. Fraser, A. L. Maier, K. R. Falchuk, and J. S. Coblyn. Long-term prospective study of methotrexate in the treatment of rheumatoid arthritis. 84-month update. *Arthritis Rheumatism* **35**:129–137 (1992).
3. J. R. Bertino. Folate antagonists: Toward improving the therapeutic index and development of new analogs. *J. Clin. Pharmacol.* **30**:291–295 (1990).
4. G. R. Westerhof, J. H. Schornagel, I. Kathmann, A. L. Jackman, A. Rosowsky, R. A. Forsch, J. B. Hynes, F. T. Boyle, G. J. Peters, and H. M. Pinedo. Carrier- and receptor-mediated transport of folate antagonists targeting folate-dependent enzymes: Correlates of molecular-structure and biological activity. *Mol. Pharmacol.* **48**:459–471 (1995).
5. B. Nuernberg, R. Koehnke, M. Solsky, J. Hoffman, and D. E. Furst. Biliary elimination of low-dose methotrexate in humans. *Arthritis Rheumatism* **33**:898–902 (1990).
6. M. Masuda, Y. I'izuka, M. Yamazaki, R. Nishigaki, Y. Kato, K. Ni'inuma, H. Suzuki, and Y. Sugiyama. Methotrexate is excreted into the bile by canalicular multispecific organic anion transporter in rats. *Cancer Res.* **57** 3506–3510 (1997).
7. H. Suzuki and Y. Sugiyama. Transporters for bile acids and organic anions. In W. Sadee and G. Amidon (eds.), *Membrane Transporters as Drug Targets,* Plenum Publishing, New York, 1999 pp. 387–439.
8. J. Konig, A. T. Nies, Y. Cui, I. Leier, and D. Keppler. Conjugate export pumps of the multidrug resistance protein (MRP) family: Localization, substrate specificity, and MRP2-mediated drug resistance. *Biochim. Biophys. Acta* **1461**:377–394 (1999).
9. K. Palm, P. Stenberg, K. Luthman, and P. Artursson. Polar molecular surface properties predict the intestinal absorption of drugs in humans. *Pharm. Res.* **14**:568–571 (1997).
10. K. Palm, K. Luthman, A. Ungell, G. Standlund, F. Beigi, P. Lundahl, and P. Artursson. Evaluation of dynamic polar molecular surface area as predictor of drug absorption: Comparison with other computational and experimental predictors. *J. Med. Chem.* **41**:5382–5392 (1998).
11. P. Stenberg, K. Luthman, and P. Artursson. Prediction of membrane permeability to peptides from calculated dynamic molecular surface properties. *Pharm. Res.* **16**:205–212 (1999).
12. E. Silla, F. Villar, O. Nilsson, J. L. Pascual–Ahuir, and O. Tapia. Molecular volumes and surfaces of biomacromolecules via GEPOL: A fast and efficient algorithm. *J. Mol. Graphics* **8**:168–172 (1990).
13. I. Tunon, E. Silla, and J. L. Pascual-Ahuir. Molecular surface area and hydrophobic effect. *Protein Engineering* **5**:715–716 (1992)
14. B. J. van Steen, I. van Wijngaarden, M. T. Tulp, and W. A. Soudijn. Series of N4-imidoethyl derivatives of 1-(2,3-dihydro-1,4-benzodioxin-5-yl)piperazine as 5-HT_{1A} receptor ligands: Synthesis and structure-affinity relationships. *J. Med. Chem.* **38**:4303–4308 (1995).
15. E. Friche, E. J. Demant, M. Sehested, and N. I. Nissen. Effect of anthracycline analogs on photolabelling of p-glycoprotein by [^{125}I]iodomycin and [^{3}H]azidopine: Relation to lipophilicity and inhibition of daunorubicin transport in multidrug resistant cells. *Br. J. Cancer* **67**:226–231 (1993).
16. J. W. Smit, E. Duin, H. Steen, R. Oosting, J. Roggeveld, and D. K. Meijer. Interactions between P-glycoprotein substrates and other cationic drugs at the hepatic excretory level. *Br. J. Pharmacol.* **123**:361–370 (1998).
17. T. Terasaki, H. Nouda, and A. Tsuji. Relationship between lipophilicity and binding affinity with human serum albumin for penicillin and cephem antibiotics. *J. Pharmacobio. Dyn.* **15**:99–106 (1992)
18. G. Coruzzi, M. Adami, C. Pozzoli, F. Giorgi, and G. Bertaccini. Cardiac and gastric effects of histamine H2 receptor antagonists: no evidence for a correlation between lipophilicity and receptor affinity. *Br. J. Pharmacol.* **118**:1813–1821 (1996).
19. A. Atke, H. Vilhardt, and P. Melin. Correlation between myo-

metrial receptor affinity, lipophilicity and antagonistic potency of oxytocin analogues in the rat. *J. Endocrinol.* **118**:187–192 (1988).
20. L. J. Bain and G. A. LeBlanc. Interaction of structurally diverse pesticides with the human MDR1 gene product p-glycoprotein. Toxicol. *Appl. Pharmacol*. **141**:288–298 (1996).
21. H. Matsuoka, N. Ohi, M. Mihara, H. Suzuki, K. Miyamoto, N. Maruyama, K. Tsuji, N. Kato, T. Akimoto, Y. Takeda, K. Yano, and T. Kuroki. Antirheumatic agents: Novel methotrexate derivatives bearing a benzoxazine or benzothiazole moiety. *J. Med. Chem.* **40**:105–111 (1997).
22. H. Matsuoka, N. Maruyama, H. Suzuki, T. Kuroki, K. Tsuji, N. Kato, N. Ohi, M. Mihara, Y. Takeda, and K. Yano. Antirheumatic agents II: Novel methotrexate derivatives bearing an alkyl-substituted benzene ring. *Chem. Pharm. Bull.* **44**:2287–2293 (1996).
23. P. C. Hirom, P. Millburn, R. L. Smith, and R. T. Williams. Species variations in the threshold molecular-weight factor for the biliary excretion of organic anions. *Biochem. J.* **129**:1071–1077 (1972).
24. F. T. Aziz, P. C. Hirom, P. Millburn, R. L. Smith, and R. T. Williams. The biliary excretion of anions of molecular weight 300-800 in the rat, guinea pig and rabbit. *Biochem. J.* **125**:25–26 (1971).